AD-A103 152 NAVAL ACADEMY ANNAPOLIS MD DIV OF ENGINEERING AND WEAPONS F/G 11/6
CORROSION FATIGUE OF ANODIZED ALUMINUM 7075-T73 IN SALT LADENED--ETC(U)
JAN 81 A T FUNKE, D F HASSON, C R CROWE

UNCLASSIFIED USNA-EW-1-81 NL

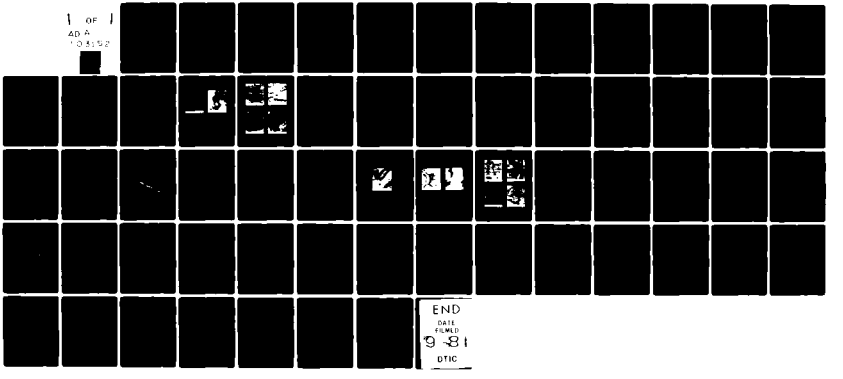

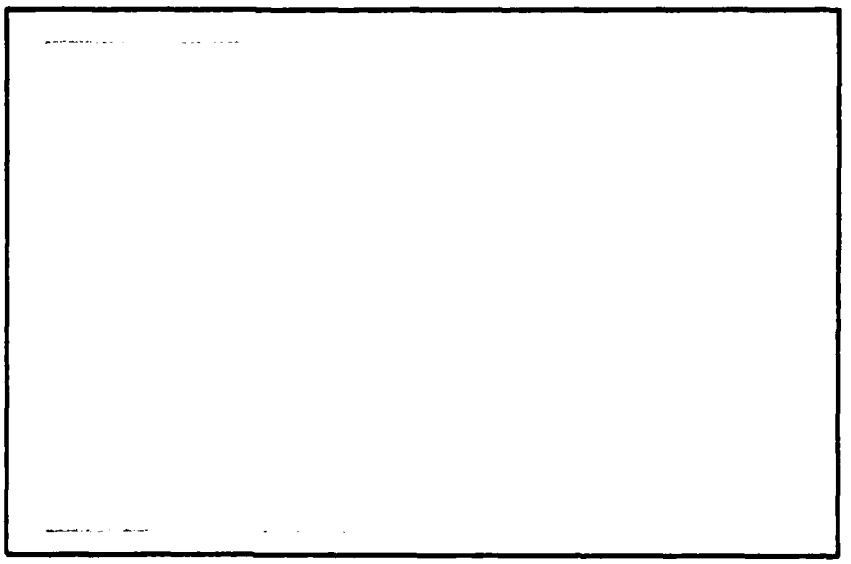

UNITED STATES NAVAL ACADEMY
DIVISION OF
ENGINEERING AND WEAPONS
ANNAPOLIS, MARYLAND

A

EW-1-81

January 1981

"Corrosion Fatigue of Anodized Aluminum 7075-T73 in Salt Ladened Humid Air"

A. T. Funke*, D. F. Hasson* and
C. R. Crowe**

*Ensign, USN and Associate Professor, respectively,
Mechanical Engineering Department
U. S. Naval Academy, Annapolis, Maryland 21402
**Naval Surface Weapons Center, Research and
Technology Department
Silver Spring, Maryland 20910

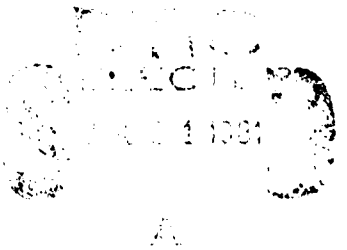

Unclassified

SECURITY CLASSIFICATION OF THIS PAGE (When Data Entered)

REPORT DOCUMENTATION PAGE		READ INSTRUCTIONS BEFORE COMPLETING FORM
1. REPORT NUMBER -EW-1-81	2. GOVT ACCESSION NO. AD-A103 152	3. RECIPIENT'S CATALOG NUMBER
4. TITLE (and Subtitle) Corrosion Fatigue of Anodized Aluminum 7075-T73 in Salt Ladened Humid Air		5. TYPE OF REPORT & PERIOD COVERED Final, Jan 80-Jan 81 6. PERFORMING ORG. REPORT NUMBER
7. AUTHOR(s) A. T. Funke D. F. Hasson C. R. Crowe		8. CONTRACT OR GRANT NUMBER(s) N60921-80-WR-W0357
9. PERFORMING ORGANIZATION NAME AND ADDRESS United States Naval Academy Division of Engineering and Weapons Mechanical Engineering Department		10. PROGRAM ELEMENT, PROJECT, TASK AREA & WORK UNIT NUMBERS 61153N WR022-01-001
11. CONTROLLING OFFICE NAME AND ADDRESS United States Naval Academy Annapolis, Maryland 21402		12. REPORT DATE January 1981 13. NUMBER OF PAGES 53
14. MONITORING AGENCY NAME & ADDRESS(if different from Controlling Office)		15. SECURITY CLASS. (of this report) Unclassified 15a. DECLASSIFICATION/DOWNGRADING SCHEDULE
16. DISTRIBUTION STATEMENT (of this Report) Unclassified - Distribution Unlimited		
17. DISTRIBUTION STATEMENT (of the abstract entered in Block 20, if different from Report)		
18. SUPPLEMENTARY NOTES		
19. KEY WORDS (Continue on reverse side if necessary and identify by block number) Corrosion Fatigue, Aluminum 7075-T73, Marine Environment, Anodization, Controlled Humidity Chamber		
20. ABSTRACT (Continue on reverse side if necessary and identify by block number) Corrosion fatigue of A17075-T73 anodized by various methods has been measured in salt laden moist air. Principal results are: (1) anodization caused a reduction in fatigue life irrespective of the thickness or type of anodization; (2) a correlation of alumina density with fatigue life was not found; (3) reduction of fatigue life in the environment is attributed to crack growth of microcracks both present and/or initiated in the anodized coating. Details of fatigue environmental chamber and statistical analysis of the data are given in appendices.		

DD FORM 1 JAN 73 1473 EDITION OF 1 NOV 65 IS OBSOLETE
S/N 0102-LF-014-6601

Unclassified

SECURITY CLASSIFICATION OF THIS PAGE (When Data Entered)

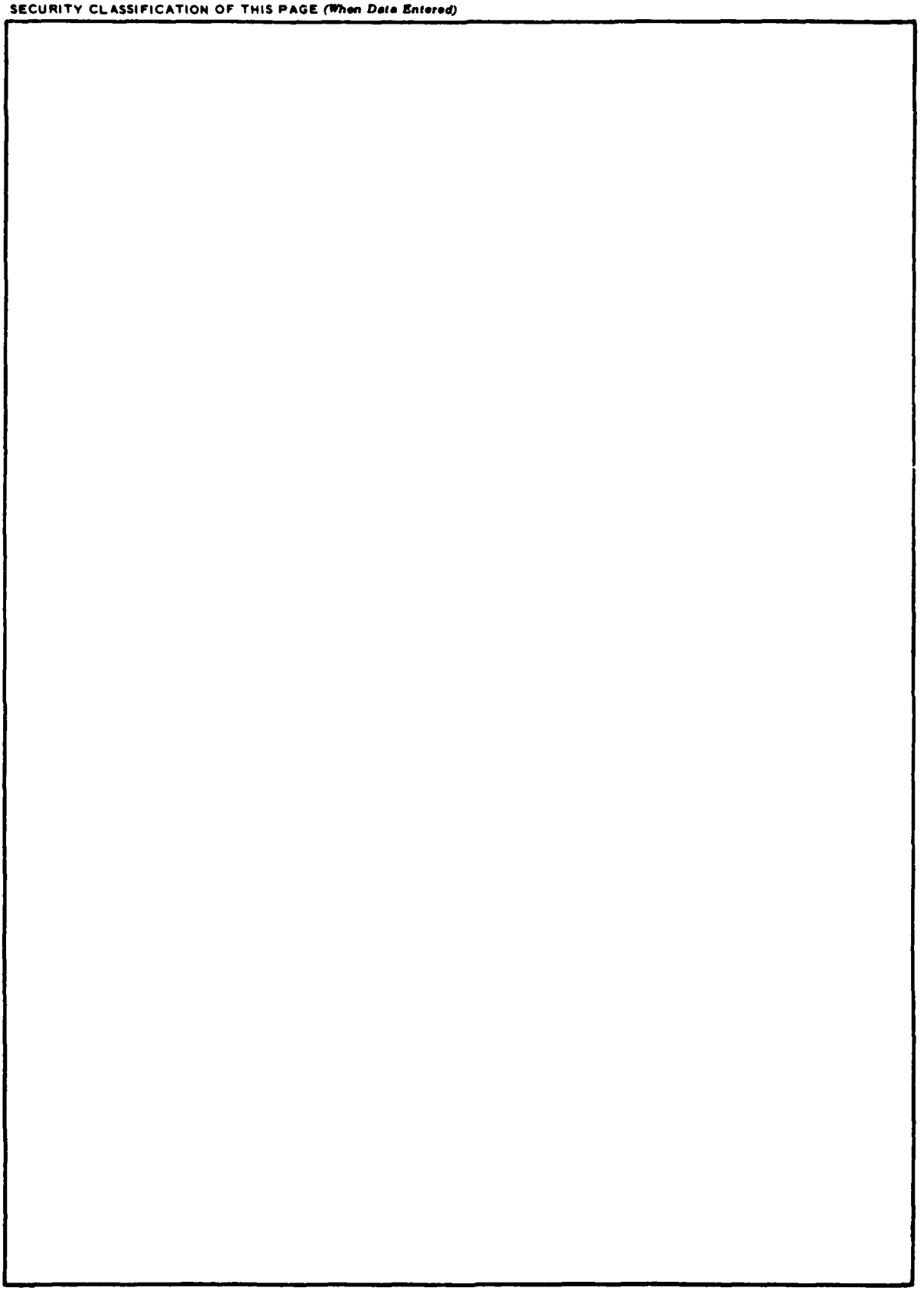

FOREWORD

The authors wish to acknowledge the laboratory support of Messrs. W. Umlandt and F. Rider. The assistance and guidance with the statistical analysis by Professor J. O. Geremia was especially helpful. The authors are indebted to Ensign Michael Young, USN for preparation of the eutectic anodized specimens.

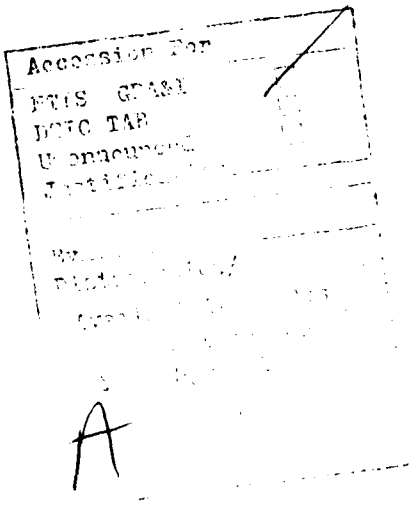

CONTENTS

TABLES

ILLUSTRATIONS

INTRODUCTION

Aluminum alloys for marine application are subjected to a corrosion environment. In structural applications such as marine aviation and ship superstructures there is the additional situation of fatigue loading. Consequently, in addition to general corrosion resistance, materials must also have corrosion fatigue resistance. General corrosion resistance is usually provided by the application of anodization or organic coatings. These coatings, especially the material-oxide or anodized types, can cause a degradation on the corrosion fatigue resistance.

Most of the previous corrosion fatigue work has been on the effect of relative humidity on the fatigue life of coated aluminum alloys. Eeles and Thurston[1] were some of the early investigators to note the effect of humidity on the fatigue life of Alcan 57S aluminum sheet. They found that different relative humidities caused different thicknesses of oxide layers, and that differences in cracking of the oxide layer could affect crack initiation in the base material.

Eeles[2] extended this work to tartaric-acid anodized Alcan 59S aluminum sheet and he noted similar degradation in the corrosion fatigue behavior. He concluded that strain discontinuities at the metal-oxide interface of the

barrier layer instead of in the outer oxide layer that was exposed to the atmosphere were the cause of fatigue failure. Eeles and Thurston[3] later studied natural oxide films on Alcan 57S and unclad 2024-T3 in moist and dry air. One of their principal observations was that thick oxide films considerably reduce fatigue life. They attributed this result to higher differential strains in the oxide encountered at the metal interface. Beitel and Bowles[4] study of the effects of anodic films on Al 1100 and high purity single-crystal aluminum, however, showed a new result. They found that although the mode of fracture is dependent on oxide thickness, the cycles to initiation and failure were independent of oxide thickness.

More recently Womack et. al[5] investigated the combined effect of relative humidity and coating thickness on the fatigue of anodized 2024-T351 aluminum in reversed torsion. They also found no effect of coating thickness on fatigue life. Coated compared to uncoated specimens, however, exhibited greater fatigue resistance at low relative humidity. Recently Simons et. al[6] have shown that the density of the anodic coating is variable with anodization techniques and therefore maybe the important characteristic for corrosion fatigue resistance. A dense coating could be thin and flexible and hence not break to become a crack initiator into the base metal. The dense coating could, therefore, significantly improve the corrosion fatigue resistance. The present study was performed to investigate this hypothesis. The effect on the corrosion fatigue life of thin and thick sulfuric acid anodized layers on Al 7075-T73 were studies to provide a comparison in coating density. Corrosion fatigue data on other dense anodization coatings, such as ammonium tartrate and potassium nitrate/lithium nitrate eutectic, are also presented. The Al 7075-T73 aluminum

alloy was selected due to its previously reported excellent corrosion fatigue and stress-corrosion resistance.[7] The present study has the additional feature of incorporating rests in a high relative humidity salt-ladened atmosphere compared to most of the previously described results in a moist atmosphere without chloride ions present.

EXPERIMENTAL DETAILS

MATERIALS.

The material tested was Aluminum 7075-T73. This is a high strength Al-Zn-Mg-Cu alloy tempered for relatively high toughness and good stress corrosion cracking resistance.[7] The material chemical composition is given in Table 1. The pre-cut form of the material was a cross-rolled 1/8 inch Al 7075 sheet in the T-6 condition. The specimen blanks were cut from the sheet in the L-S direction, then milled to meet the geometry, as shown in Figure 1, for a standard bending fatigue test.

The microstructure of the Al 7075-T73 sheet is shown in Figure 2. In Figure 2(a) surface scratches and pores and inclusions can be seen. In Figure 2(b) the specimen cross-section which was etched by Keller's reagent shows a relatively small grain size. The microstructure is nearly single phased with inclusions inside the grains. Energy dispersive x-ray scans of the inclusions showed them to be aluminum depleted and iron and copper rich. Zinc and magnesium were not concentrated in these inclusions, but were detected as uniformily distributed in the matrix.

TABLE 1 COMPOSITION LIMITS FOR Al 7075-T73

COMPOSITION

ELEMENT	PER CENT	
	MIN	MAX
COPPER	1.2	2.0
MAGNESIUM	2.1	2.9
MANGANESE	–	0.30
IRON	–	0.7
SILICON	–	0.50
ZINC	5.1	6.1
CHROMIUM	0.18	0.40
TITANIUM	–	0.20
OTHER IMPURITIES		
EACH	–	0.05
TOTAL	–	0.15
ALUMINUM	BALANCE	BALANCE

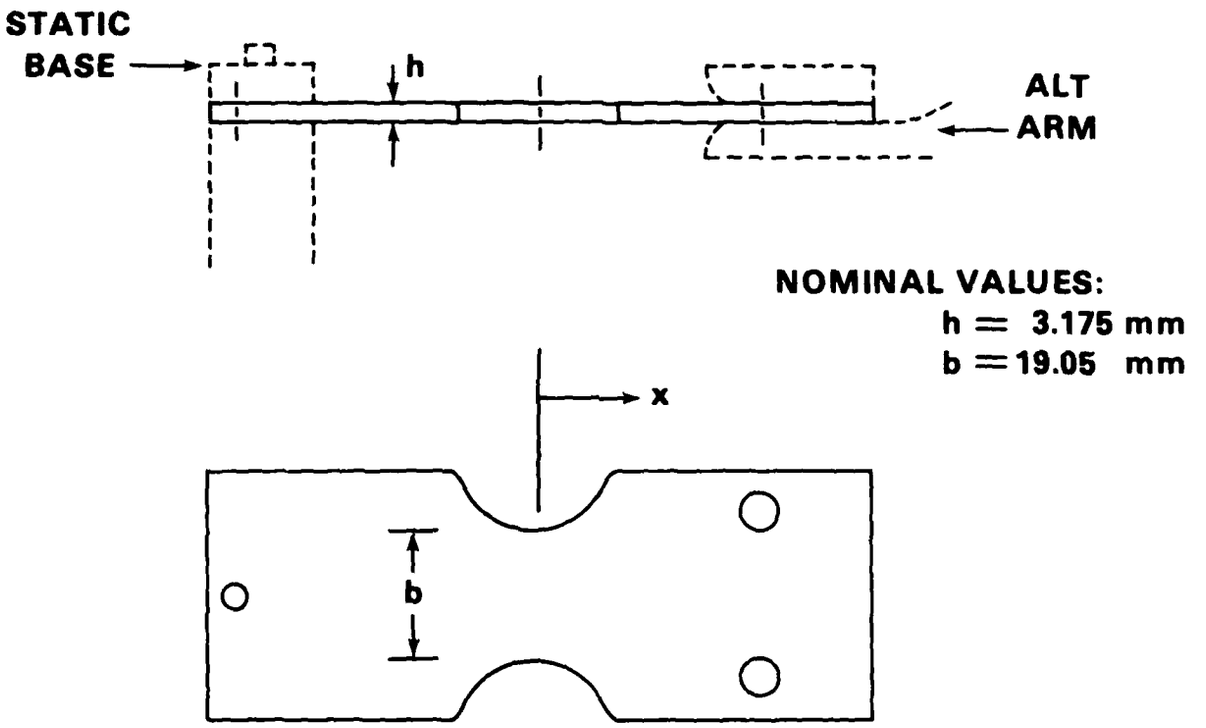

Figure 1 Test Specimen

ANODIZATION TREATMENTS.

After the samples were machined to size, the T-73 temper was accomplished by heating in a pre-heated furnace for 9 hours at 177°C, and then air cooling to room temperature. The samples were then chemically etched by dipping in a solution of 180 ml H_3PO_4, 75 mil H_2SO_4, and 9 ml HNO_3 at 95° for 10 seconds. They were then dipped in a desmutting solution and cleaned with distilled water.

The samples requiring a 0.4-0.5 micron thick ammonium tartrate [$(NH_4)_2C_4H_4O_6$] coating were anodized in a glass beaker between two platinum electrodes. The platinum electrodes were made cathodic and the sample anodic. Ammonium tartrate anodizing was performed at 1 ma/cm^2, so the samples were anodized at 78 ma, with the voltage increasing from 0 volts to 200 volts. Upon reaching 200v, the samples were removed and cleaned with distilled water and ethanol.

The samples requiring a thick (9.9 micron) sulfuric acid (H_2SO_4) anodized layer were anodized with a current density of 13 ma/cm^2 for 20 minutes at 18-layer 20 volts. The cathode was made of lead. The coated samples were then sealed in boiling water, as is the method commonly used in industry today.

The thin (0.4-0.5 micron) H_2SO_4 anodized layer was applied with platinum electrodes as the cathode. The current density was 13 ma/cm^2, and the time required was 60 seconds at a voltage of 18-20 volts. The coated samples were then cleaned with distilled water and ethanol.

The samples prepared in a eutectic salt mixture consisting of 65 w/o potassium nitrite and 35 w/o lithium nitrate (65 w/o KNO_2 and 35 w/o $LiNO_3$) were anodized at 127°C in an aluminum tube, which served as cathode. A 3.25 ampere current was held for 60 seconds resulting in a 7.9 micron thick oxide layer. The eutectic anodized samples were then cleaned in distilled water and ethanol.

Micrographs of the anodized surfaces are shown in Figure 3. Figure 3(a) for the thin sulfuric acid coating shows that the coating does not cover the inclusions, noted in Figure 2(a), of the as received surface. Figure 3(b) shows that the thick sulfuric acid anodized layer has its own structure and contains porosity. Figure 3(c) for the ammonium tartrate coating is similar in appearance to the thin sulfuric acid layer shown in Figure 3(a). The surface roughness markings also can be seen in the micrograph. The eutectic coating, shown in Figure 3(d), exhibits numerous cracks and some porosity.

FATIGUE MACHINE.

Two fatigue machines were used for testing the specimens. Both machines are Sonntag SF-2-U bending fatigue machines by Wiedemann Baldwin Division of the Warner and Seansey Company. The operating frequency was 1800 rpm (30 Hertz), and each 1000 cycles of stress were recorded by a mechanical counter. The alternating load (constant amplitude) was applied using an off-center revolving weight in which the eccentric distance could be increased to increase the load. Although the machines had the capability of applying a mean load as well, only purely alternating bending loads were used for these experiments.

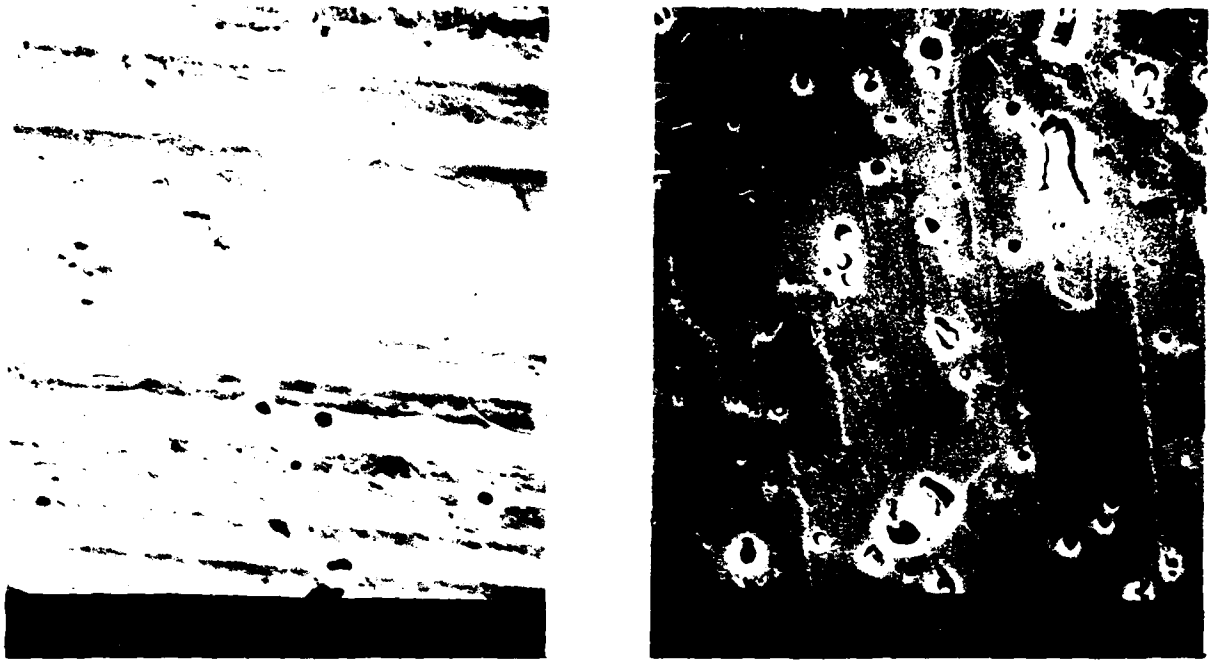

Figure 2 Untreated Al 7075-T73 (a) Surface and (b) Cross Section Microstructures (1000X)

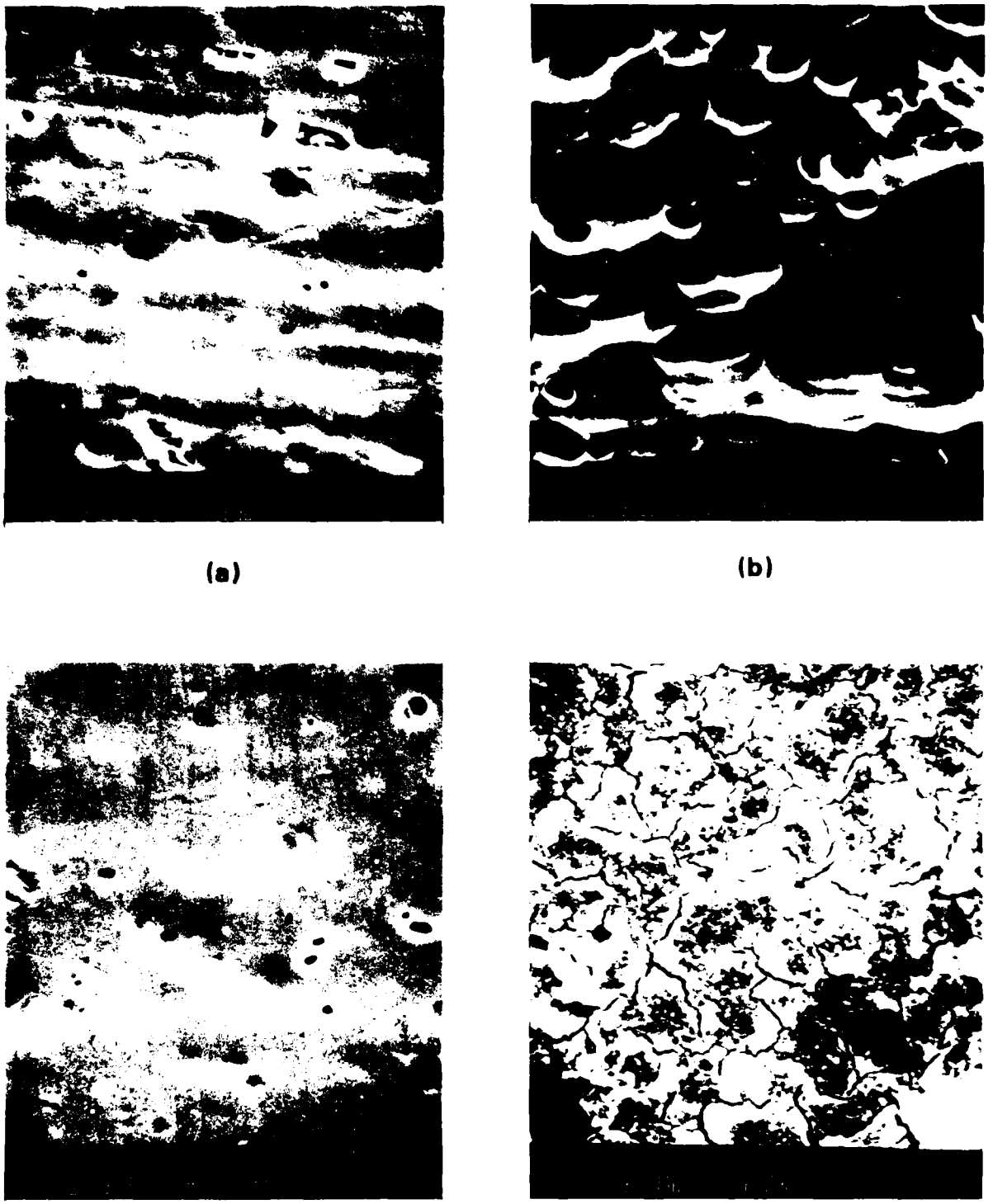

Figure 3 SEM Surface Micrographs of (a) thin sulfuric acid, (b) thick sulfuric acid (c) ammonium tartrate and (d) eutectic coatings (1000X).

In order to obtain accurate stress values, the fatigue machine was calibrated. Several calibration methods were used to compare against each other. The procedure selected consisted of calibrating the mean load spring with a Vishay-strain indicator (Wheatstone Bridge), and then calibrating the dynamic load to the static load spring by using a TEKTRONIX 475 oscilloscope and a bridge amplifier.

The relationship between the spring-equivalent load (S) and the Wheatstone Bridge calibrated load (W) was found to be

$$W = .92\ (S) - .05 \tag{1}$$

The relationship between the spring-equivalent load (S) and the dynamic-dialed load (D) was found to be

$$S = 1.056\ (D) + .04056 \tag{2}$$

Combining equations (1) and (2):

$$W = .92\ [1.056(D) + .04056] - .05 \tag{3}$$

or,

$$W = .972\ (D) - .013 \tag{4}$$

In other words, 10 pounds load dialed into the dynamic load will produce a real load of 9.71 pounds. This is using the Wheatstone Bridge load as the reference. If it is assumed that the spring constant of the fatigue machine remains constant even after several years of use, which is usually considered a valid assumption, the relationship

$$S = 1.056\ (D) + .04056 \tag{5}$$

shows that the 10 pounds dialed into the dynamic load is actually 10.6 pounds load. However, because each of the above testing devices showed approximately 5% scatter in their results, it was assumed that the dialed-in and the actual applied load were the same.

The failure criterion used for each fatigue test was either complete fracture of the specimen or a weakening of the material to such a degree that the amplitude of the constant amplitude load machine increases to a point where the machine turns itself off.

SPECIMEN PREPARATION.

All the anodized samples (ammonium tartrate, thick sulfuric acid, thin sulfuric acid, and eutectic) were dipped in a 3.5 w/o NaCl solution and allowed to dry in lab air for one-half hour. The untreated base-line samples were not salt dipped and the relative humidity for these samples was that of lab air (43% relative humidity and 24^{o}C).

After the anodized specimens were salt dipped, they were placed in an environmental chamber designed to reach a relative humidity (RH) of 91% at about room temperature. A schematic of the chamber is given in Figure 4. Other chamber designs are described in Appendix A. The potassium sulfate solution consisted of approximate 300 ml of K_2SO_4 and H_2O solution, thus assuring complete saturation with K_2SO_4 at the surface of the solution. The heating tape at the base of the chamber was used to reduce the reaction time of the solution so that 91% RH could be reached in approximately 1.5 hours. An electric hygrometer indicator (EHI) by Hygrodynamics, Inc. was used to monitor the %RH in the chamber. An ultra-thin surgical glove thumb was used for the air tight boot shown.

CORROSION FATIGUE PROCEDURE.

The different types of test specimens were run at dynamically applied loads of 85.4, 64.0, and 42.7 N, resulting in nominal reverse bending stress levels of 322, 241, and 161 MPa, which corresponds to .70, .52 and .35 of the 0.2% offset yield stress. The applied mean load was always zero for each test.

For the initial testing, four specimens were tested at each stress level for each of the five different surface conditions. Using the results of this testing, the sample size needed for a 99% confidence of 5% or less error at each stress level was determined using a method by Lipson and Sheth[8]. The numbers of samples required by this method were 4, 7 and 6 data points at each of the 322, 241, and 161 MPa stress levels, respectively. At the stress levels where more than the initial four data points were required, more specimens were tested.

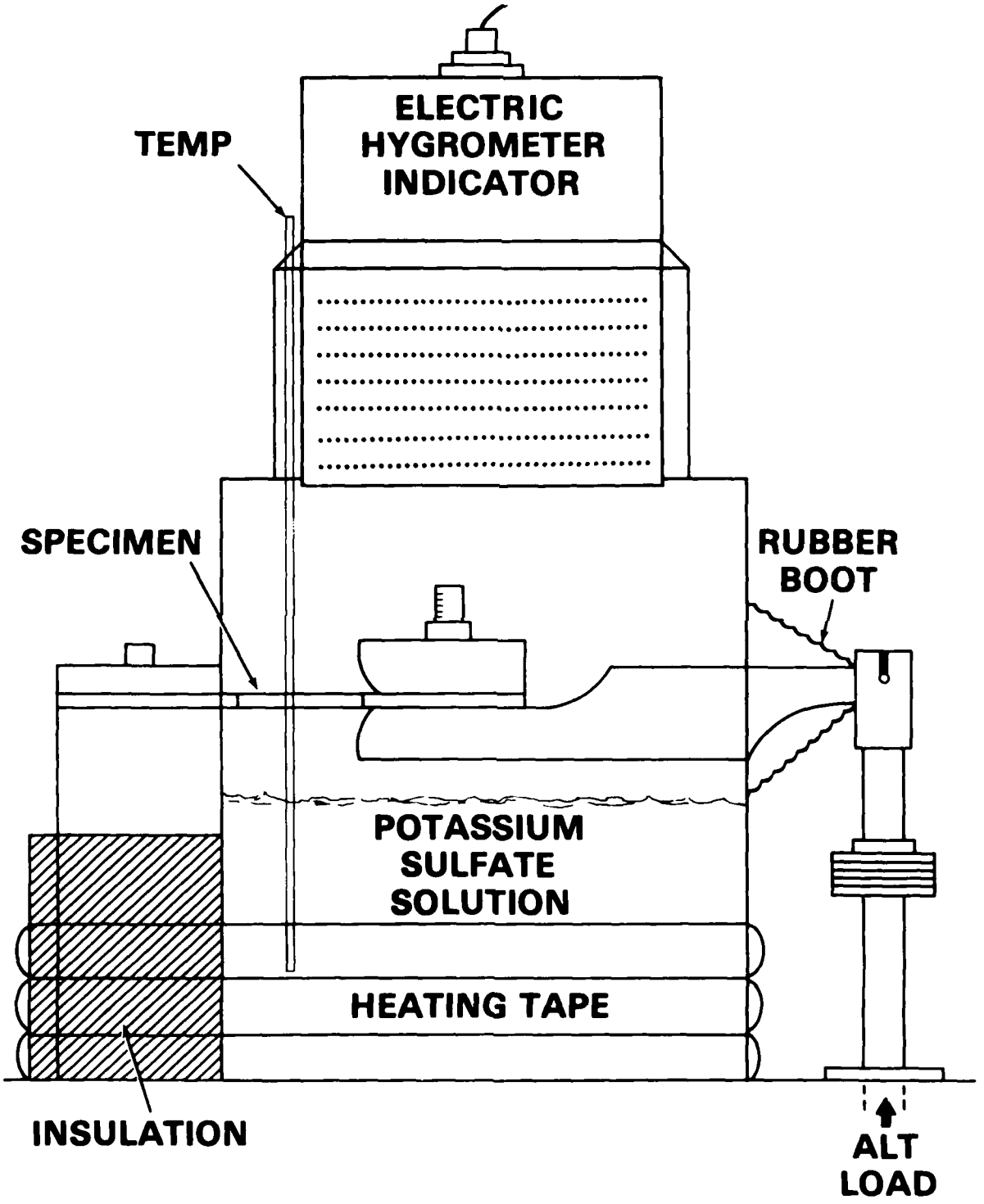

Figure 4 Corrosion Fatigue Test Environmental Chamber

RESULTS AND DISCUSSION

FATIGUE TESTS.

The results of the fatigue and corrosion fatigue tests are presented in Tables 2 thru 6. The values for the cycles to failure were obtained from the mechanical counter on each machine. The alternating stresses shown were calculated from the applied alternating load, the area at the fracture, and the moment distance from the point of load application to the fracture using the equation

$$\sigma_a = \frac{Mc}{I} \tag{6}$$

where M = the moment created by the alternating load and is equal to the load times the moment distance,

and C = distance from neutral axis to outer fiber which is one-half of the height of the cross-section,

and I = the cross-sectional moment of inertia.

So $$\sigma_a = \frac{(P_{app})(d)(\frac{h}{2})}{(\frac{bh3}{12})}$$

or $$\sigma_a = \frac{6(P_{aap})(d)}{bh^2} \tag{7}$$

TABLE 2 S-N DATA FOR Al 7075-T73, UNTREATED SURFACE IN LAB AIR AT 43%RH AND 24°C

RUN NUMBER	APPLIED ALTERNATING STRESS (mPa)	CYCLES TO FAILURE (10^3 CYCLES)
1	318.0	11
4	321.8	15
5	320.9	14
12	318.8	11
2	241.3	47
6	213.5	63
8	239.5	39
11	241.6	47
13	243.0	53
14	240.7	47
15	240.6	54
3	156.6	203
7	160.4	214
9	140.7	733
10	160.6	204
16	160.6	262
17	160.6	282

TABLE 3 S-N DATA FOR Al 7075-T73 AMMONIUM TARTRATE COATING, IN SALT LADEN AIR AT 91%RH AND 25°C

RUN NUMBER	APPLIED ALTERNATING STRESS (mPa)	CYCLES TO FAILURE (10^3 CYCLES)
1	318.5	9
4	325.2	7
13	320.5	9
14	322.7	9
2	239.4	26
8	241.8	23
9	214.8	46
10	237.7	25
15	208.7	59
16	238.5	31
17	241.2	26
18	236.2	26
3	159.3	140
5	159.0	199
6	140.7	240
11	158.4	202
12	160.7	176
19	154.9	190

TABLE 4 S-N DATA FOR Al 7075-T73, THICK SULFURIC ACID COATING, IN SALT LADEN AIR AT 91%RH AND 25°C

RUN NUMBER	APPLIED ALTERNATING STRESS (mPa)	CYCLES TO FAILURE (10^3 CYCLES)
1	321.8	7
4	280.6	8
8	321.4	6
11	323.5	6
13	321.1	7
3	239.7	20
5	240.4	18
7	241.0	19
10	212.2	59
16	208.2	42
17	235.6	33
18	215.6	45
2	158.7	168
6	156.0	131
9	140.7	461
12	160.7	181
14	160.8	163
15	159.8	157

TABLE 5 S-N DATA FOR Al 7075-T73, THIN SULFURIC ACID COATING, IN SALT LADEN AIR AT 91%RH AND 25°C

RUN NUMBER	APPLIED ALTERNATING STRESS (mPa)	CYCLES TO FAILURE (10^3 CYCLES)
1	315.4	5
2	320.1	5
11	320.9	5
12	321.6	7
5	244.7	20
6	241.7	20
7	212.9	24
8	239.7	46
15	239.1	26
16	240.0	23
18	231.0	21
3	161.8	154
4	159.8	130
9	160.2	153
10	159.8	134
13	158.3	262
14	139.9	163

TABLE 6 S-N DATA FOR Al 7075-T73, EUTECTIC COATING, IN SALT LADEN AIR AT 91%RH AND 25°C

RUN NUMBER	APPLIED ALTERNATING STRESS (mPa)	CYCLES TO FAILURE (10^3 CYCLES)
1	322.5	8
8	317.6	7
9	314.6	8
17	278.9	11
4	227.4	32
5	239.1	22
12	229.9	29
13	237.0	35
14	237.4	33
15	241.2	30
16	240.5	30
2	157.6	161
3	160.6	624
6	161.8	431
7	160.4	212
10	138.6	649
11	159.3	331

where P_{app} = Applied alternating load

d = moment distance [in Figure 1, d = (12.1-X) cm]

b = base of fracture

h = height of fracture area

The alternating stress values for the fatigue data plotted as a function of cycles to failure are shown in Figure 5. Each of the five sets of data were fitted to the equation

$$Y = AX^B \tag{8}$$

This particular equation was chosen, because the error of the data about the line was low when compared with that of other equations. Also it yields a straight line on a log-log plot. The stress versus number of cycles to failure curves in Figure 3 represent a 50% confidence level. The following observations can be made from the data:

a. The effect of anodizing the specimens was to lower the fatigue life at a given alternating stress, especially at the high stress level. Since other anodized Al 7075-T73 corrosion fatigue data especially in salt ladened moist air is not available in the open literature, the present level of degradation cannot be compared.

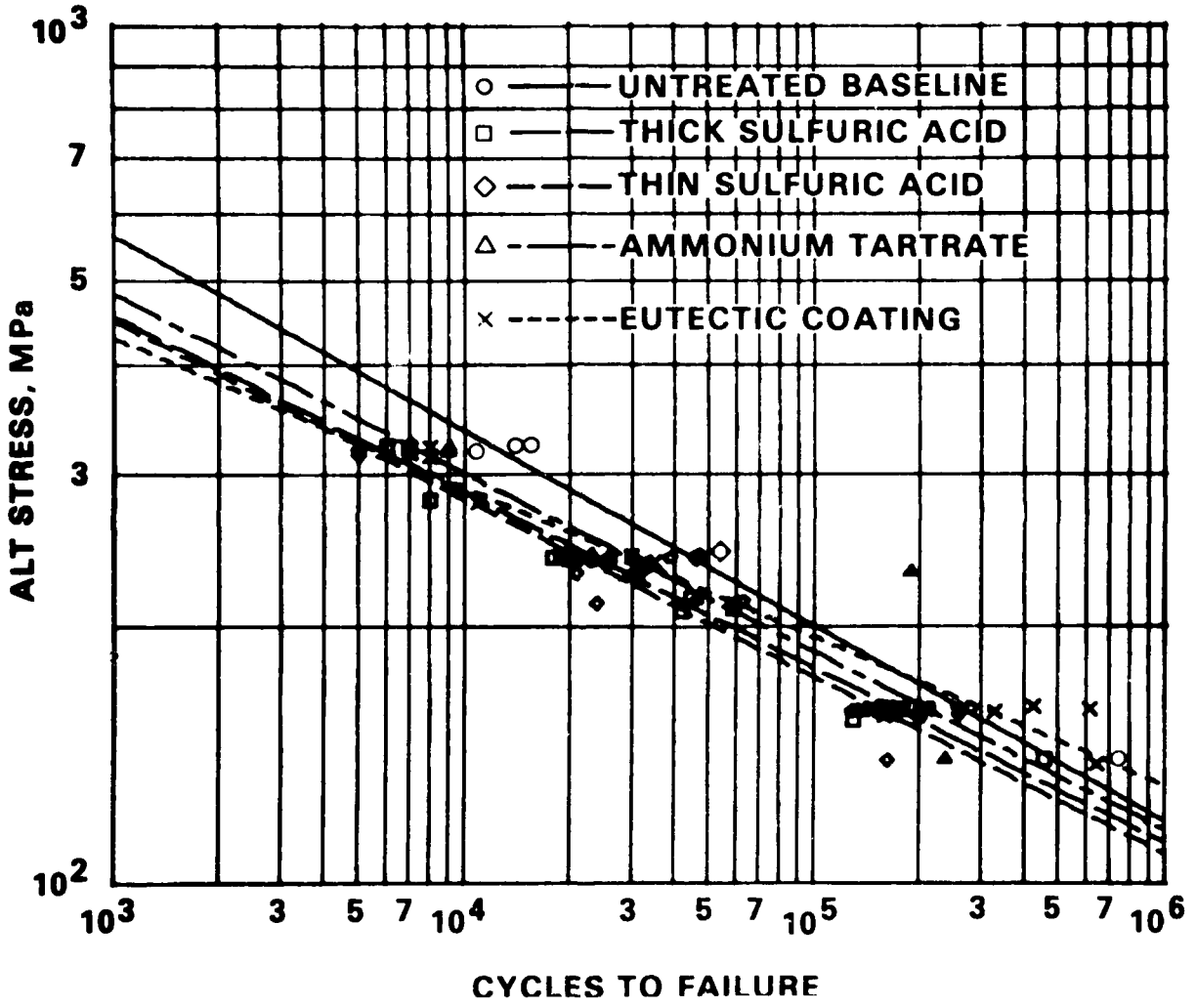

Figure 5 Alternate Stress Versus Cycles to Failure For Corrosion Fatigue. Tests on Un-and Various Anodized Al 7075-T73 Sheet Specimens

b. Comparison of the thin and thick sulfuric acid coatings data showed no effect on the corrosion fatigue life.

c. The ammonium tartrate coated specimens had better corrosion fatigue resistance than did the sulfuric acid coated specimens.

d. The eutectic coated specimens had the shortest fatigue life at the high stress, but at the medium stress they had the longest life of the coated specimens. At the low stress level the eutectic coated specimens had a longer fatigue life than even the untreated, baseline specimens.

These observations were based on the 50% confidence curve fitting the fatigue data. When the confidence level was increased to 95%, a statistical analysis described below proves that there is no significant statistical difference between the five data sets.

To statistically compare the data, equation (8) was made linear, resulting in

$$\log (Y) = B \log (x) + \log (A) \qquad (9)$$

which gives slope B and intercept = log (A). Using a standard line comparison method as outlined by J. O. Gerenia[9], the standard error of the slope and the standard error of the intercept were determined. Details of the statistical analysis are given in Appendix B. These errors were used in conjuction with the two-tailed student t-test to obtain the 95% confidence intervals about the slope

value and about the intercept value. These intervals for one set of data were then compared with similar intervals for another set of data. If both the slope intervals for each line and the intercept intervals for each line overlaped, then it was concluded that there was no significant difference between two lines at the 95% confidence level.

Using this statistical analysis at the 95% confidence level, the only significant difference between any of the five curves was between the uncoated and the eutectic curve. This was only at alternating stresses in excess of 2/3 of the yield stress where the uncoated samples had a longer life than the coated samples.

FRACTOGRAPHY.

Scanning electron microscope (SEM) fractography was performed on the various specimen failure cross sections and surfaces. A typical failure cross-section SEM fractograph from an untreated specimen is shown in Figure 6. Since the cross section represented the bulk specimen properties and not the surface layer, the quasi-cleavage type fracture surface with inclusions and striation markings is typical for both untreated and anodized specimens.

Surface SEM fractographs of the surface of the untreated specimen are given in Figure 7. Even though the surface is untreated, it appears to have a thin surface layer, perhaps Al_2O_3 formed by surface oxidation. A microcrack and even smaller cracks appear at what appear to be at the boundaries on an untested specimen shown in Figure 2(a). The higher magnification fractograph in Figure

7(b) shows very fine microcracks in the surface which could be the source of the larger surface cracks also shown in the fractograph.

Surface SEM fractographs for tested anodized specimens are shown in Figure 8. Cracks caused by tension in the anodized surfaces are apparent for all surface treatments. The thick sulfuric acid anodized surface, Figure 8(b), also show microcracks at various directions relative to the surface tensile axis. This is probably due to cracking of the thick brittle layer. Since there was no difference in the corrosion fatigue behavior between thick and thin sulfuric acid treatments, the hypothesis about increasing the density of the coating could be questioned. However, even though more porosity and microcracks could be in an unstressed thick coating, coating thickness is not directly related to coating density. The present study, therefore, did not prove or disprove the hypothesis.

Cracking in the eutectic coating, Figure 8(d) seemed to follow the boundaries of the already existing discontinuities shown in Figure 3(d) which appears to be a non-uniform coating.

CONCLUSIONS

The following observations were made:

a. Thin and thick sulfuric acid, ammonium tartrate and potassium nitrite/lithium nitrate eutectic anodization treatments caused a reduction in the fatigue life of Al 7075-T73 sheet. The cause is attributed to the crack growth of microcracks both present and/or initiated in the anodized coating.

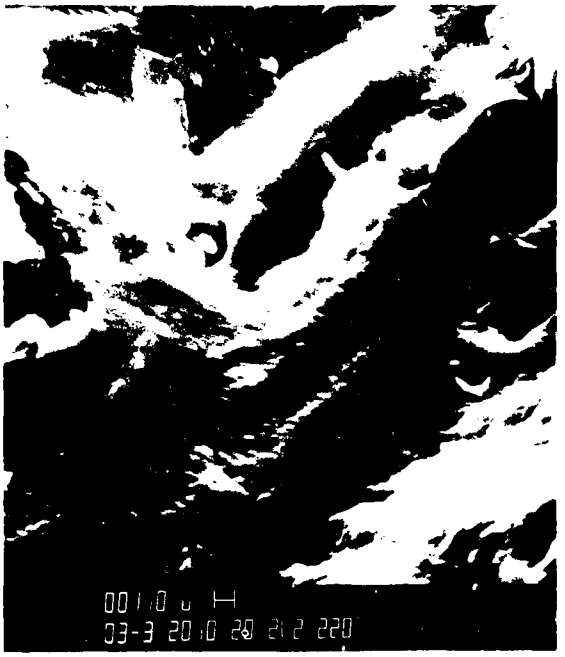

Figure [illegible] alternating

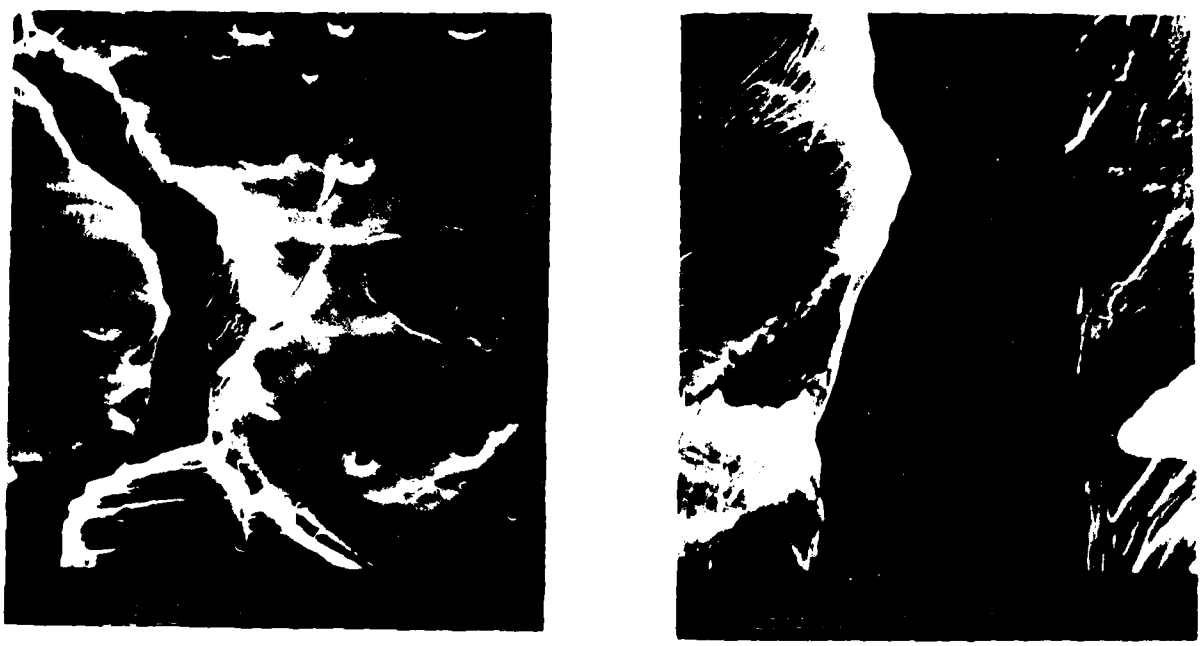

(a)

Figure 7 SEM Surface Fractograph of Untreated Al 7075-T3 Tested at 320 MPa Alternating Stress (a) 1000X and (b) 5000X.

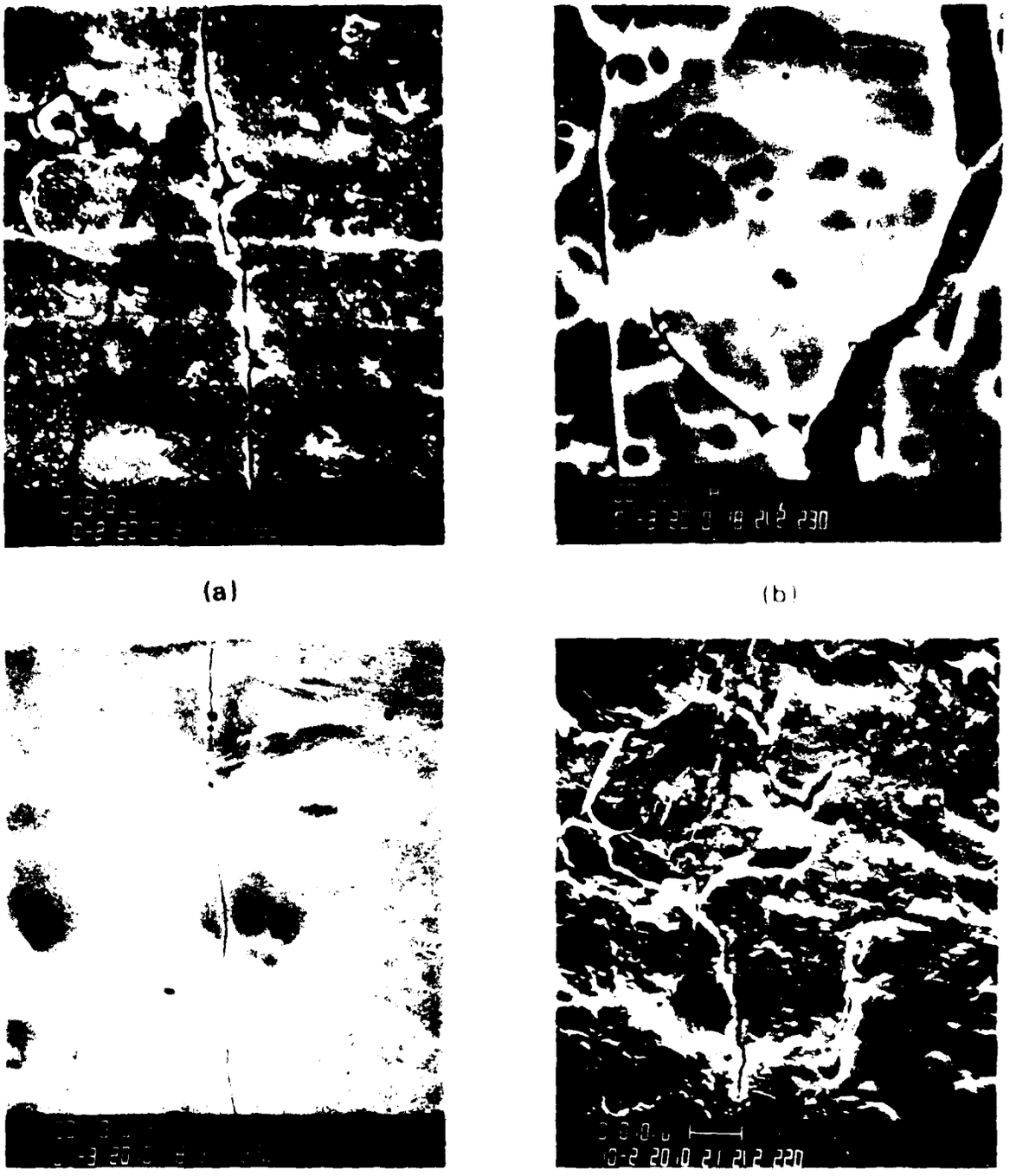

[illegible] Surface fractographs of (a) [illegible]
Chromic Acid, (c) Ammonium Tartrate and
[illegible] tested at 320 MPa [illegible]

b. Based on a 95% confidence level statistical analysis, there was no difference in the corrosion fatigue behavior for any of the coatings.

c. Due to the lack of open literature information on corrosion fatigue behavior especially in salt ladened moist air of un - or anodized Al 7075-T73 sheet, a comparison of the present results was not possible.

d. Due to the thin and thick sulfuric acid coatings yielding the same fatigue life results, the hypothesis that increased anodized layer density should improve corrosion fatigue behavior is somewhat in question. Thin or thick coatings per se, however, do not infer different coating densities, and the present study does not prove or disprove the increased density hypothesis.

REFERENCES

1. Eeles, E. G. and Thurston, R. C. A., "The Relation of Humidity to the Fatigue Endurance of An Aluminum Alloy," J. Inst. Metals, 95, 111-115 (April 1967).
2. Eeles, E. G., "The Effect of Thin Anodic Oxide Films on the Fatigue Behavior of an Aluminum Alloy," J. Inst. Metals, 95, 115-157 (May 1967).
3. Eeles, E. C. and Thurston, R. C. A., "Atmosphere and Surface Effects and the Fatigue of Aluminum Alloys," AIAA Journal 8 (2), 22-4-228 (Feb 1970).
4. Beitel, G. A. and Bowles, C. Q., "Influence of Anodic Layers on Fatigue-Crack Initiation in Aluminum," Metal Science Journal, 5,85-91 (May 1971).
5. Womack, E. F., Wilson, J. H. and Mabie, H. H. "Torsional Fatigue Tests of Anodized Aluminum Rods," Experimental Mechanics, 362-368 (Oct 1976).
6. D. G. Simons, C. R. Crowe, M. D. Brown, H. DeJarnette, D. S. Land, and J. G. Brenhan, J. Electrochem Soc., 123, 2558 (1980).
7. Nordmark, G. E., Lifka, B. W., Hunter, M. S., and Kaufman, J. G., "Stress-Corrosion and Corrosion Fatigue Susciptibility of High-Strength Aluminum Alloys," Technical Report AFML-TR-70-259, AD720857, (November 1979).
8. Lipson, C. and Sheth, N. J., Statistical Design and Analysis of Engineering Experiments, McGraw Hill Book Company, pp 264-270, (1973).
9. Geremia, J. O., Private Communication, 1980.

APPENDIX A

SELECTION OF A HIGH HUMIDITY CHAMBER

Several methods for obtaining high humidity for a fatigue testing chamber were attempted before a suitable design was attained. The original basis for obtaining high humidity inside the chamber was the American Society for Testing of Materials (ASTM) method described in E104, "Maintaining Constant Relative Humidity by Means of Aqueous Solutions."[A1] The original humidity chamber, as shown in Figure A1, was designed to meet the requirements stated in ASTM E104 in terms of the ratio of volume above the liquid surface to the area of the liquid surface.

Theoretically, by housing a saturated solution of potassium sulfate (K_2SO_4) in an enclosed or slightly vented chamber, a relative humidity (RH) of 96.5% can be maintained at any constant temperature over a temperature range of 20-40^{o}C. A maximum volume of the air space per unit area of surface of solution of 25.4 cubic centimeters per square centimeter was recommended. The original chamber, with the saturated solution inside, had a free air volume of 1427.3 cm^3 and a solution surface area of 68.4 cm^2. This gave a ratio of 21.0 cm_3/cm_2, well within the ASTM recommendation. Temperature fluctuations were kept to a minimum by operating at room temperature and using thermally insulated Lucite as the chamber material. Thus, 96-97% RH was expected, but the

DEPTH OF CHAMBER = 85 mm

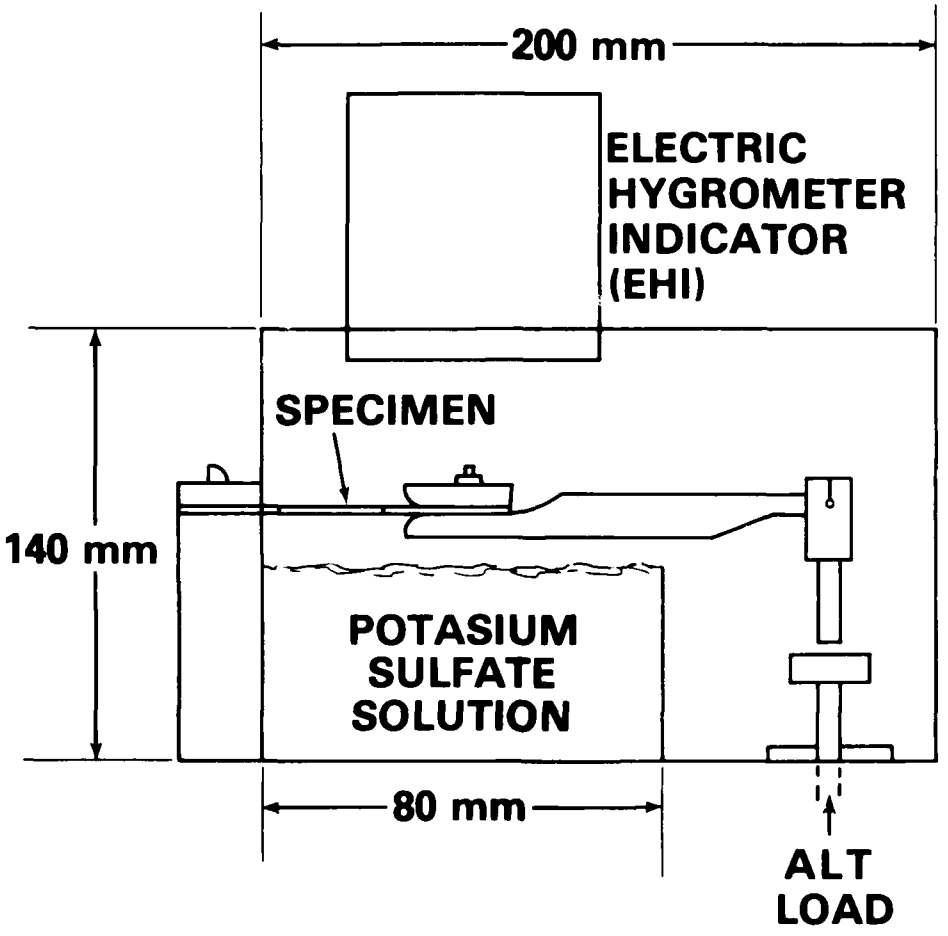

FIGURE A1 ORIGINAL CHAMBER

relative humidities measured by the electric hygrometer indicator (EHI) were, at best and over the period of the test, approximately 75% R.H. Thus, an alternate method was necessary to maintain a high humidity for the duration of each fatigue test. This method must be repeatable and, if possible, have a reasonable conditioning time.

First, the free air volume to solution surface area was reduced from 21.0 cm^3/cm^2 to less than 5 cm^3/cm^2. A 600 ml stainless steel beaker was used to house the EHI and the saturated K_2SO_4 solution for testing the effect of the reduced ratio. A 90% RH was reached, but the time required to reach this level varied from 2.5 to 18 hours, which is not repeatable and too time consuming.

A static air chamber seemed to be desirable over a dynamic flow chamber. With air flow into and out of the chamber, a more precisely monitored control system would be necessary and the air flow across the specimen would add yet another undesirable variable to the whole test procedure. However, if 95-100% RH could be piped into the chamber by slow, natural convection, accomplished by heating the K_2SO_4 solution in a remote beaker, the disadvantages of a dynamic system might be minimized. Thus, the design shown in Figure A2 was built. The high RH air also has a chance to cool back down to room temperature (RT) before entering the chamber. This system did show some success, but it was inconsistent in obtaining high humidity readings.

Another dynamic humidity chamber system was attempted with the use of a heated bubble tower (Fig. A3). This chamber reached 95.9 RH in a short time,

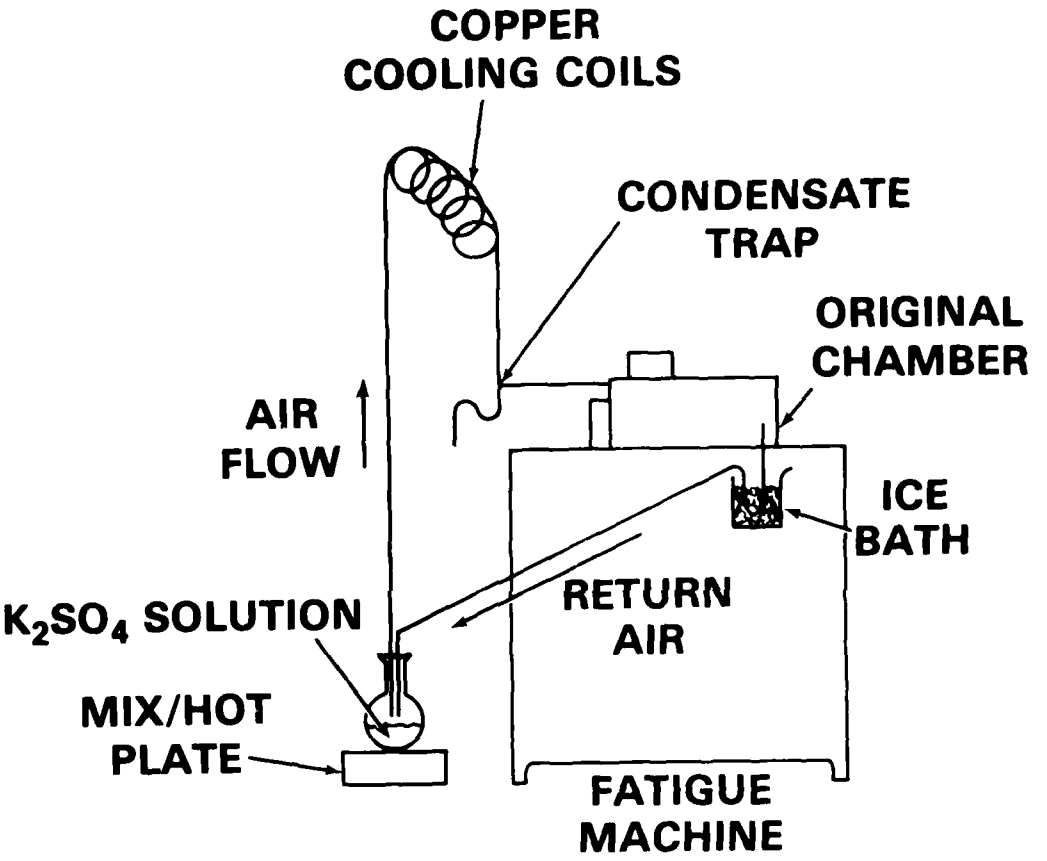

FIGURE A2 NATURAL CONVECTION DYNAMIC CHAMBER SYSTEM

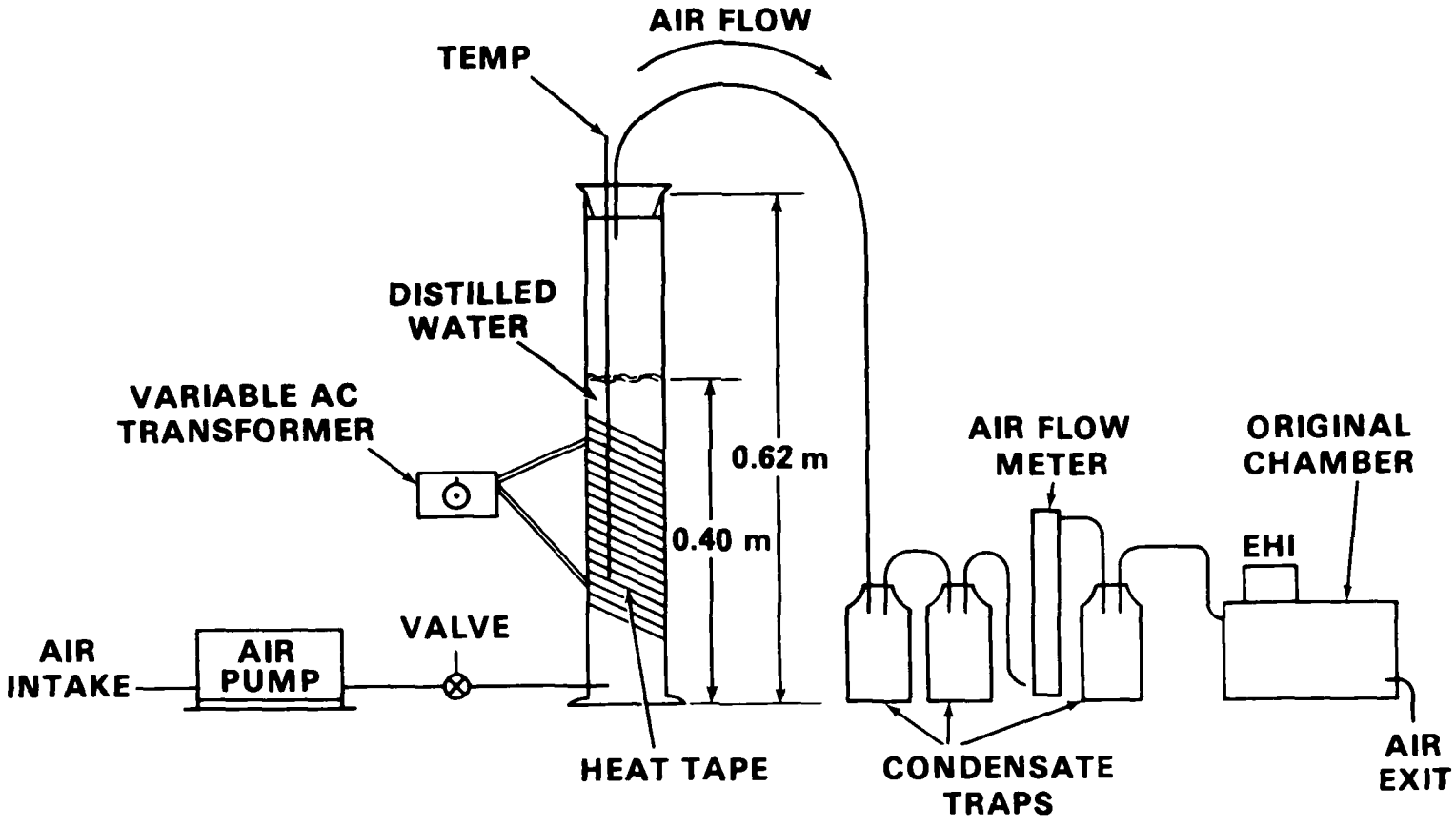

FIGURE A3 BUBBLE TOWER CHAMBER SYSTEM

but required an air flow of approximately 5 liters/min, which was undesirable, so a better system was sought.

In working on the natural convection dynamic system (Figure A2), it was found that if the solution was heated to 3-5°C above RT while the free air lagged behind at approximately 1-3°C above RT, a high humidity could be reached in a short time. From this idea combined with the lower free air volume to surface area ratio came the design for the chamber that meets the high humidity fatigue test requirements.

The free air volume in original chamber was reduced by eliminating the half of the chamber that did not have any solution in it. A flexibile boot, cut from the thumb of an ultra-thin disposable rubber surgical glove, was used to seal the chamber where the loading arm extends through it. This decreased the ratio from 21 to 5 cm^3/cm^2. Three feet of heating tape was wound around the base of chamber to heat the solution. Finally, the K_2SO_4 solution was made up so as to have more than half of the liquid volume taken up by K_2SO_4 precipitate. This maintains complete saturation at the solution surface, according to F. C. Quinn,[A2] who has done extensive research in the area of using aqueous solutions to obtain high relative humidity. All the above design consideration were used in building the chamber utilized herein. Figure A4 shows a schematic of this chamber.

The selected chamber could consistently maintain 91% RH after approximately 1.5 hours of preparation time. There was no air flow across the specimen, and the air temperature remained at 26 + 2°C. For tests which last longer than

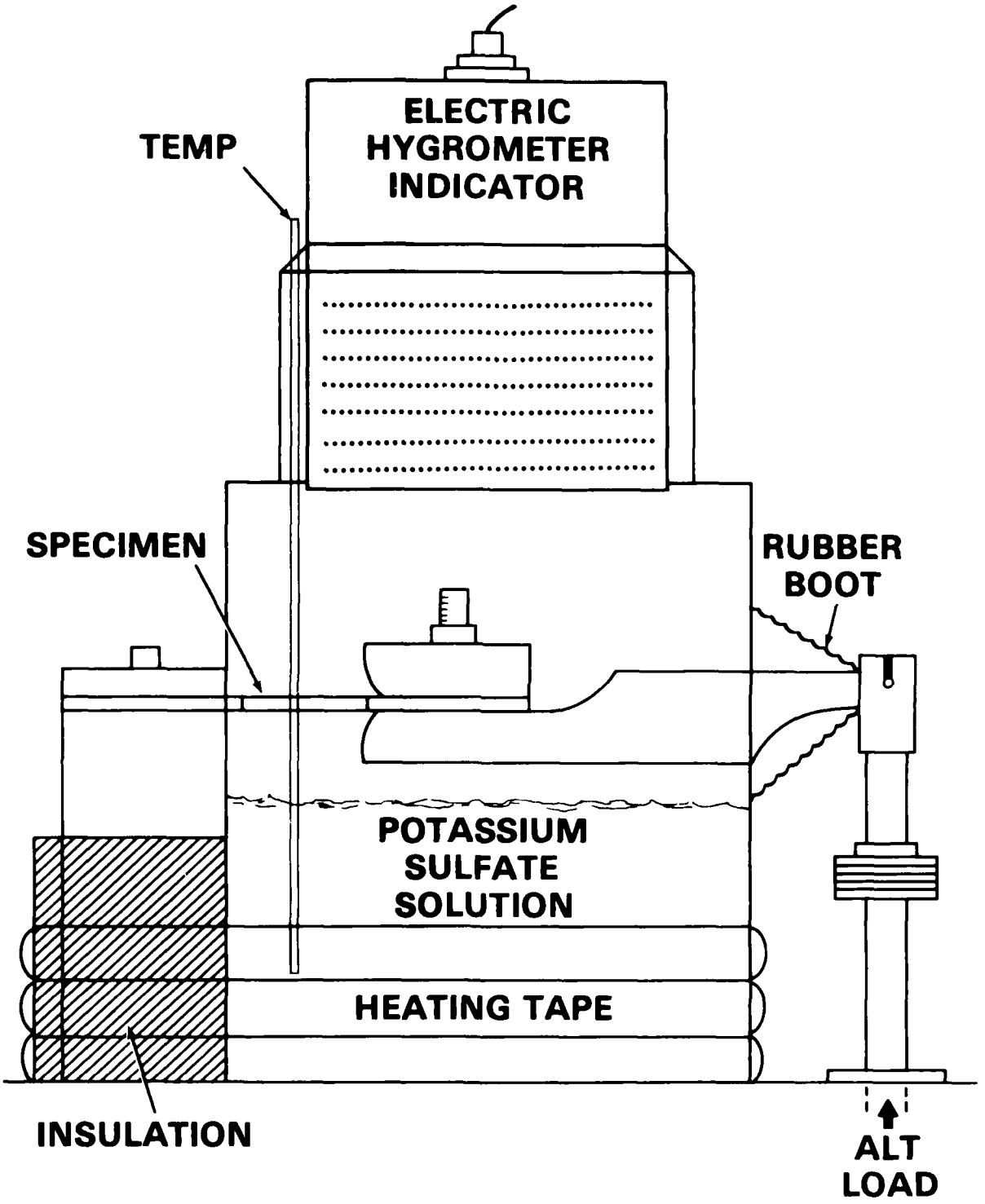

FIGURE A4 CORROSION FATIGUE TEST ENVIRONMENTAL CHAMBER

ten hours, the solution heat input may have to be monitored and controlled. This heat increase or decrease could possibly be controlled with the application of a hygrometer controller with a relay switch mechanism. For the zero to three hour long tests of this experiment, this small, heated chamber satisfactorily provided the required % RH at an essentially constant temperature.

REFERENCES

A1 1976 Annual Book of ASTM Standards, part 35, E104, pp831-834.

A2 Hygrodynamics Technical Bulletin No. 5, "Creating and Maintaining Humidities by Salt Solutions."

APPENDIX B

STATISTICAL ANALYSIS OF THE FATIGUE DATA

Fatigue datam because of its sensitivity to surface finish conditions and internal inhomogeneties has a large amount of scatter. It can not be simply represented by any one mathematical model. These reasons have left fatigue data representation to a mere fairing of a curve to fit the data. The resulting curve has only a 50% confidence level. To compare one set of fatigue data with another at a high confidence level, however, requires more than a mere curve faring. First, a mathematical model must be found which best fits the data. Then, a high confidence level statistical analysis is needed to best compare this model with another model which has been fit to a second set of fatigue data taken from another material condition (such as a different surface finish).

When the fatigue data is taken at specific constant stress amplitudes, such as at 2/3, 1/2, and 1/3 of the yield stress, a logarithmic average can be taken at each stress level and a curve fitted between these averages.[B1] Assuming a log-normal distribution of fatigue data[B2], confidence level intervals can be drawn at each stress level. Because of the relatively small sample size, the student "t" test must be used to obtain the two boundary points of the confidence intervals at each stress level. Connecting these points, each curve will have a scatter band. Determination of a statistical difference can then be

made visually by comparing this with another set of line data. The scatter bands show where or if the two sets overlap (see Figure B1). This technique has several drawbacks, however, because it relies on the sometimes crowded usual comparisons instead of using an accepted formal comparison. Also, if the fatigue test is such that many stress amplitudes are applied, the determination of separate confidence intervals at each stress level becomes unreasonable.

An accepted formal comparison of the two sets of data can be made by first choosing an equation by which to model the data so that the variance of the data about the line will be low. This equation can then be linearized with the use of logarithms, and a formal comparison can be made of the slope and of the intercept with those of another similarly reduced set of data.

If either the slopes or the intercepts show a significant difference, then the lines can be shown to be different. If two lines have equal slopes and different intercepts, then one line is significantly higher than the other. If the lines have significantly different slopes, then the lines will be significantly different except at the portion where both lines intersect. Making a formal comparison between the slope and the intercept of two lines has been described by J. O. Geremia.[B3] His method was used herein, and will be described in an example comparison.

First, to choose an equation which fits the data well, all five sets of data were fit to several equations using the method of least squares. The variance about each equation was determined by calculating r^2, the coefficient of determination for a line:

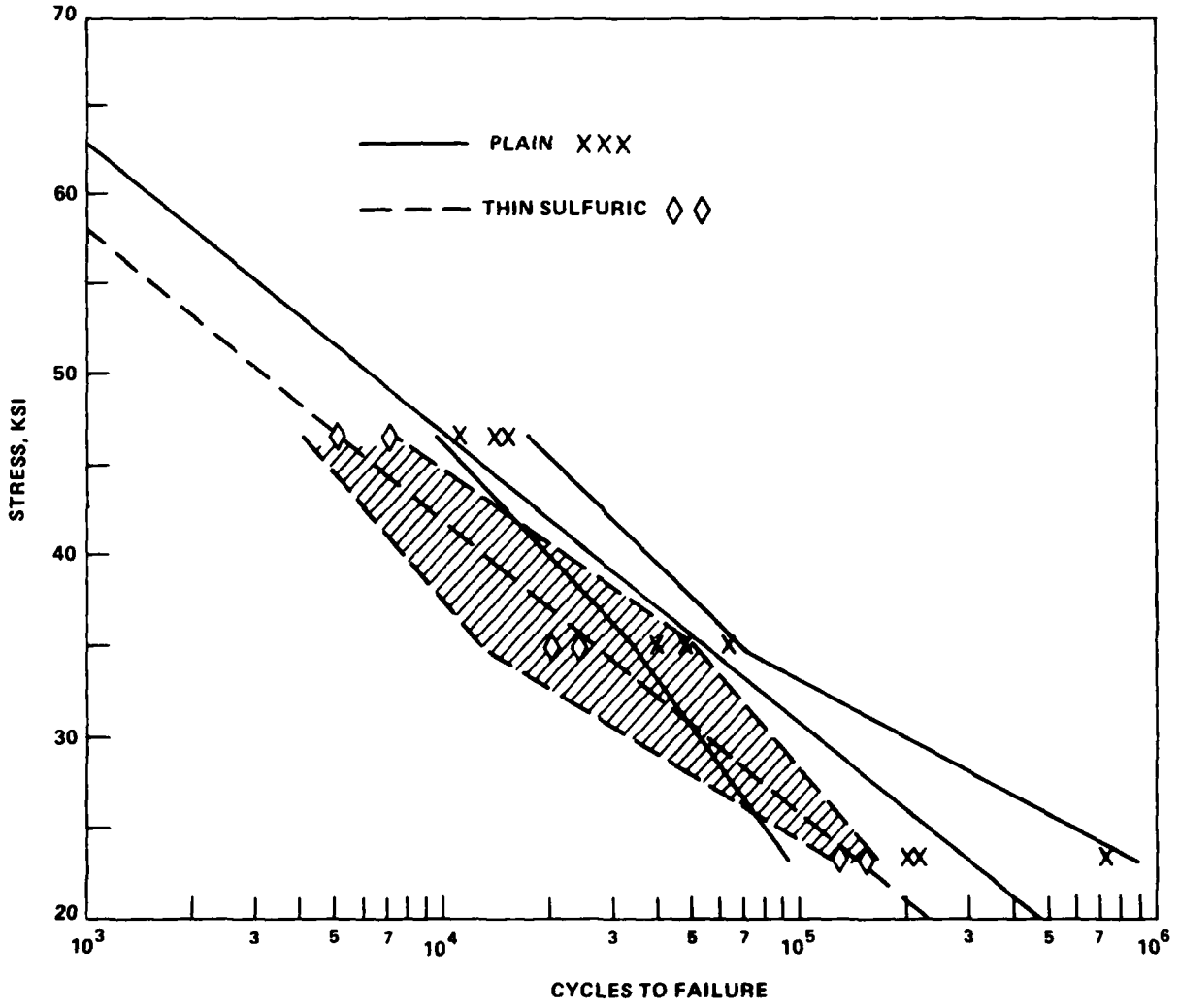

FIGURE B1 PLAIN VS THIN WITH 95% SCATTER BANDS

$$r^2 = 1 - \frac{\Sigma(Y_i - Y_{Pi})^2}{\Sigma(Y_i - Y)^2} \qquad \text{(B1)}$$

To calculate r^2, the line must first be made linear (by the use of logarithms). For example, if the fatigue data equation is

$$Y = A\ X^B \qquad \text{(B2)}$$

where Y is the stress (in MPa) and X is the cycles (in cycles) and A and B are constants, it can be made linear to equal

$$\text{Log}\ (Y) = \text{Log}\ (A) + B\ \text{Log}\ (X) \qquad \text{(B3)}$$

Equation (3) would then be used to calculated r^2, and the terms Y_i and X_i defined below, are actually log (stress) and log (cycles):

Y_i = value of Y for every i^{th} data point

Y_{Pi} = predicted value of Y, for the X value at every i^{th} data point, which is obtained by the linearized equation in use.

using Equation (3) for an example,

$$Y_{Pi} = a + B\ X_i$$

where $a = \log A$

and X_i = the value of X at every data point and

and finally, from Equation (1), the last linearized term needed to solve for r^2 is

$\bar{Y}$ = the average, or mean, of the Y_i values of the particular set of data:

$$\bar{Y} = \frac{\sum_{i=1}^{n} Y_i}{n} \tag{B4}$$

where n = the number of data points in the particular set of data. Again, if Y is used to analyze example Equation (B3), Y_i would be equal to log (stress).

The coefficient of determination, r^2, was used to help decide which equation should be used to model these five sets of fatigue data. Table B1 lists the three best equations and their r^2 values. The equation

$$Y = A\,X^B \tag{B5}$$

was chosen because of its high r^2 values and because it plots a straight line on log-log paper.

In this example comparison, we will use equation (5) to model the fatigue data sets of the untreated baseline specimens and of the thin sulfuric acid coated (thin) specimens, and then compare the slopes and the intercepts of the two linearized forms of equation (5).

TABLE B1 EQUATION PARAMETERS

SPECIMEN TYPES AND PARAMETER VALVES ↓ / EQUATION FORM WITH COEFFICIENTS A, B, AND C: →		Y = A + B LOG (X)	Y = A X^B	Y = A + B·LOG (X) + C·LOG(X)
UNTREATED	r^2 =	0.958364	0.972617	0.979326
	A =	281.199	2666.11	1520.23
	B =	−49.8219	−0.224916	−183.38
	C =	–	–	5.9617
THICK H_2SO_4	r^2 =	0.951857	0.975189	0.976516
	A =	701.211	1843.02	1391.3
	B =	−45.0233	−0.202485	−177.26
	C =	–	–	6.23067
THIN H_2SO_4	r^2 =	0.945416	0.947658	0.955699
	A =	704.109	1856.98	1166.45
	B =	−45.744	−0.20517	−135.949
	C =	–	–	4.32929
AMMONIUM TARTRATE	r^2 =	0.87456	0.875556	0.912831
	A =	724.692	2001.99	1871.68
	B =	−46.3521	−0.205915	−263.185
	C =	–	–	10.1207
EUTECTIC	r^2 =	0.926313	0.953924	0.979086
	A =	628.977	1419.54	1528.16
	B =	−37.139	−0.171997	−201.338
	C =	–	–	7.35163
AVERAGE r^2 VALUES	=	0.931342	0.944989	0.96069

To compare the slope of one line with the slope of another, a confidence interval must be found for each slope. If the two confidence intervals overlap, then the two slopes have no significant difference. To determine the confidence intervals, the standard error in the slope must be calculated. This value can then be used in conjunction with the two-tailed t-test (selected because of the small sample size) to determine the slope confidence intervals. The same technique is used to determine confidence intervals for the two intercepts to be compared. The standard error in the slope,

$$S_{bi} = \frac{S_{Yi}}{[\Sigma(X_i-X)^2]^{1/2}} \tag{B6}$$

where S_{Yi}, the standard error of the line estimate,

$$S_{Yi} = \left[\frac{\Sigma(Y_i-Y_{pi})^2}{n-z}\right]^{1/2} \tag{B7}$$

and X = the mean, or average, of all the X_i terms in the particular set of data,

$$X = \frac{\sum_{i=1}^{n} X_i}{n}$$

and X_i, Y_i, Y_{pi}, and n have been defined previously. All values are of the linearized form of equation (5), (which is equation (3).

The standard error of the intercept,

$$S_{bo} = S_{yi} \left(\frac{\Sigma X_i^2}{n\Sigma(X_i - \bar{X})^2} \right)^{1/2} \qquad (B8)$$

Table B2 was used to simplify evaluation and summation of the terms

$$(Y_i - Y_{Pi})^2 \quad ,$$

$$(X_i - \bar{X})^2 \quad ,$$

and X_i^2.

Now, using the results from Table B2, we will evaluate the standard errors of the untreated, baseline data.

Equation (7):

$$S_{Yi} = \left(\frac{0.006839}{17-2} \right)^{1/2}$$

$$S_{Yi} = 0.02135$$

Equation (6):

$$S_{bi} = \frac{0.02135}{[4.802]^{1/2}}$$

$$S_{bi} = 0.009744$$

Equation (8):

$$S_{bo} = 0.02135 \left(\frac{399.8}{(17)(4.802)} \right)^{1/2}$$

$$S_{bo} = 0.04726$$

TABLE B2 UNTREATED, BASELINE FATIGUE DATA REDUCING VALUES

CYCLES (10^3)	STRESS (mPa)	Xi = LOG(CYCLES)	Yi = LOG(STRESS)	$(Yi - Y_{P_1})^{2*}$	$(Xi - X)^2$	$(Xi)^2$
11	318.0	4.04	2.50	–	0.61	16.33
15	321.8	4.18	2.51	–	0.42	17.44
14	320.9	4.15	2.51	–	0.46	17.19
11	318.8	4.04	2.50	–	0.61	16.33
47	241.3	4.67	2.38	–	0.02	21.83
63	213.5	4.80	2.33	–	–	23.03
39	239.5	4.59	2.38	–	0.05	21.08
47	241.6	4.67	2.38	–	0.02	21.83
53	243.0	4.72	2.39	–	0.01	22.32
47	240.7	4.67	2.38	–	0.22	21.83
54	240.6	4.73	2.38	–	0.01	22.40
203	156.6	5.31	2.19	–	0.24	28.17
214	160.4	5.33	2.21	–	0.26	28.41
223	140.7	5.87	2.15	–	1.09	34.40
204	160.6	5.31	2.21	–	0.24	28.19
262	160.6	5.42	2.21	–	0.36	29.36
282	160.6	5.45	2.21	–	0.40	29.71
			Σ =	0.006839	4.802	399.8

* FOR TABULATION PURPOSES, THIS QUANTITY WAS TOO SMALL TO LIST. HOWEVER, THE COMPUTER SUMMATION OBTAINED THE VALUE SHOWN AT THE BOTTOM OF THE COLUMN.

Using standard two-tailed t-test tables at 95% confidence and (n-2) degrees of freedom, the slope confidence interval is

$$B \pm (t_{.95,n-2})Sb_1 \tag{B9}$$

and the intercept confidence interval is

$$\log A \pm (t_{.95,n-2})S_{b_o} \tag{B10}$$

where A and B are the constants from the equation (5), and are listed in Table B1.

Substituting values into equations (9) and (10), the slope confidence interval is equal to:

$$-0.2249 \pm (2.131)\ (0.009744)$$

or $$-0.2249 \pm 0.02076 \tag{B11}$$

and the intercept confidence interval is equal to:

$$3.426 \pm (2.131)\ (0.04726)$$

or $$3.426 \pm (0.1007) \tag{B12}$$

combining results (11) and (11), the line with 95% confidence intervals is now

$$Y = (-0.2249 \pm 0.02076)\ X \pm (3.426 \pm 0.1007) \qquad (B13)$$

with Y and X being linearize values log (stress) and log (cycles). Using the same technique for the thin data, the line equation with 95% confidence intervals is

$$Y = (-0.2025 \pm 0.02788)\ X + (3.266 \pm 0.1272) \qquad (B14)$$

Thus, equations (16) and (17) show that there is no significant difference between the slopes nor the intercepts of the two lines. Therefore, there is no statistical difference between these two data sets. The inference is, on the basis of this fatigue test, the thin sulfuric acid coating does not effect the corrosion fatigue life of Al 7075-T73.

The results of the other sets of fatigue data are in Table B3. The euctectic coating showed a significant difference with the baseline but only at stresses in excess of 2/3 the yield stress. All other data, at 95% confidence level, showed no significant difference.

TABLE B3 EQUATIONS AND CONFIDENCE INTERVALS USED IN COMPARISON OF THE FATIGUE DATA

SPECIMEN TYPE	EQUATION AND VARIANCE
UNTREATED	$Y = (3.426 \pm 0.1007) + X\ (-0.2249 \pm 0.0208)$
THICK H_2SO_4	$Y = (3.266 \pm 0.0789) + X\ (-0.2025 \pm 0.0081)$
THIN H_2SO_4	$Y = (3.266 \pm 0.1272) + X\ (-0.2025 \pm 0.0279)$
AMMONIUM TART	$Y = (3.301 \pm 0.4222) + X\ (-0.2059 \pm 0.0867)$
EUTECTIC	$Y = (3.149 \pm 0.1719) + X\ (-0.1720 \pm 0.0360)$

REFERENCES

B1 C. Lipson and N. J. Sheth, Statistical Design and Analysis of Engineering Experiments, McGraw-Hill, 1973, p266.

B2 P. H. Wirsching, J. E. Kempert, "A Fresh Look at Fatigue," Machine Design, May 20, 1976.

C. Lipson and N. J. Sheth, Statistical Design and Analysis of Engineering Experiments (above), p265.

B3 J. O. Geremia, "Design of Experiments," 1979, Mech. Eng. Dept., USNA, p68-85.

DISTRIBUTION

	Copies
Commander Naval Sea Systems Command Attn: SEA-62R (Kinna) Washington, DC 20362	1
Commander Naval Air Systems Command Attn: AIR-52031	1
AIR-52032	1
Washington, DC 20361	
Commander Naval Materials Command Washington, DC 20361	1
David W. Taylor Naval Ship R&D Center Attn: Materials Department Annapolis, MD 21402	1

DISTRIBUTION(Cont.)

	Copies
Naval Weapons Center Attn: Library China Lake, CA 93555	1
Naval Construction Battalion Civil Engineering Laboratory Attn: Materials Division Port Hueneme, CA 93043	1
Naval Air Development Center Attn: J. DeLuccia, Code 302 Warminster, PA 18974	1
Naval Postgraudate School Attn: Mechanical Engineering Dept. Prof. J. Perkins Monterey, CA 93940	1
Defense Documentation Center Cameron Station Alexandria, VA 22314	2


DA
FILM